

## Powder-Filled Semisolids: Influence of Powder Addition to Vaseline on the Rheological Properties

Shigeyuki ISHIKAWA,\* Masao KOBAYASHI and Masayoshi SAMEJIMA

Products Formulation Research Laboratory, Tanabe Seiyaku Co., Ltd., 16-89, Kashima 3-chome, Yodogawa-ku, Osaka 532, Japan.  
Received September 12, 1988

To evaluate the influence of solid particles on the rheological properties of semisolids, 6 inorganic powders classified as follows were added to vaseline; 1) fine and rigid powders (ZnO, TiO<sub>2</sub>), 2) porous powders (hydrated silicon dioxide (Cp), synthetic aluminum silicate (SiAl)), and 3) lubricating powders (talc, magnesium stearate (StMg)). Rheological measurements were performed by the oscillation method and continuous shear method.

As determined by the oscillation method, the profiles of storage modulus ( $G'$ ), loss modulus ( $G''$ ), and loss tangent ( $\tan \delta$ ) vs. powder concentration ( $f_p$ ) varied from powder to powder. In group 1,  $\log G'$ 's increased monotonously on addition of ZnO, whereas they were scarcely changed at low  $f_p$  but increased gradually at high  $f_p$  in the case of TiO<sub>2</sub>. This difference seemed to be caused by a difference in their affinity for vaseline. In group 2,  $\log G'$ 's changed only a little at low  $f_p$  but increased rapidly at higher  $f_p$ . In group 3, StMg showed the characteristic effect that it reduced  $G'$  at  $f_p$  values below 0.3.

Most of the powders gave maximum values of  $\tan \delta$  at a powder volume fraction ( $\phi_p$ ) below 0.04, and these peaks were presumed to reflect the beginning of structure formation.

As determined by the continuous shear method, porous powders (group 2) increased the apparent viscosity at high shear rate ( $\eta_{625}$ ) but the other powders did not increase  $\eta_{625}$  so much. This suggests that the structures formed by porous powders were resistant to shear but those formed by other powders were not.

**Keywords** powder; vaseline; powder filled semisolid; rheology; powder property; oscillation method; continuous shear method

### Introduction

In the previous paper, we reported that the oscillation method with nonlinear analysis proposed by Onogi *et al.*<sup>1)</sup> was applicable to some pharmaceutical semisolids.<sup>2)</sup> In this method, rheological parameters such as storage modulus ( $G'$ ), loss modulus ( $G''$ ), and loss tangent ( $\tan \delta$ ) were calculated from the linear region of the stress curve, and the method can be applied to many kinds of pharmaceutical semisolids exhibiting nonlinearity in viscoelastic measurement.

However, the relationship between the rheological parameters obtained by this method and the structures formed in a semisolid or the pharmaceutical qualities (pharmacological efficiency, acceptability in use, ease of production and so on) has not yet been well clarified. So, systematic researches on many vehicles are desirable.

In the case of viscoelastic materials,  $G'$  and  $G''$  should be regarded as indexes of solidity and liquidity, respectively. But, solidity and liquidity are based on rheological concepts and would not necessarily correspond to the compositions of solid or liquid materials contained in the vehicle. For example, in simple ointment in JP XI made from beeswax and soybean oil,  $\tan \delta (=G''/G')$  increased in spite of the increase of solid material (beeswax), and this corresponds to an increase in the relative contribution of liquidity,<sup>2)</sup> whereas  $\tan \delta$  of carboxyvinylpolymer gel containing only 1% polymer showed lower  $\tan \delta$  than that of simple ointment containing a large amount of solid materials.<sup>3)</sup> Thus, the rheological properties of semisolids should depend greatly on the nature of the structure formed by the solid materials rather than on the fraction of solid materials.

Therefore, it would be useful to know the influence of powders having various properties on rheological properties and the relation between the structures formed in the semisolid and the powder properties, from both basic physicochemical viewpoints and practical standpoints, in

order to get ointments having desirable consistency.

Rheological studies on the influence of solid particles added to viscoelastic materials have been carried out in many fields, and many experimental or theoretical equations have been proposed. However, little work has been reported on pharmaceutical semisolids. Recently, Radebaugh and Simonelli evaluated the rheological properties of powder-filled semisolids using lanolin as the matrix phase and ZnO, colloidal sulfur, and potato starch as the dispersed phase.<sup>4)</sup> This research is suggestive, but seems to be insufficient from the practical viewpoint, because lanolin has particular viscoelastic properties and is not a common vehicle for ointments, and their study was not designed to elucidate a systematic relationship between the rheological properties of powder-filled semisolid and the powder properties.

In this paper, we used vaseline, which is one of the most common vehicles used for ointments, and added 6 inorganic powders having various properties (ZnO, TiO<sub>2</sub>, hydrated silicon dioxide (Cp), synthetic aluminum silicate (SiAl), magnesium stearate (StMg), talc) and glass beads (as a control). The 6 powders are commonly used in ointment or cosmetic formulations.

For rheological evaluation, the oscillation method which measures at the rheological ground state and the continuous shear method using a Ferranti-Shirley viscometer which measures at higher shear rates were used.

On the basis of the results, the presumable structures formed by individual powders and the influence of the structure on the rheological properties are discussed.

### Experimental

**Materials** All materials were obtained from commercial sources. The vaseline used in the paper was of JP XI grade and of moderate consistency (white petrolatum Protopet 1S, Witco Chemical Co.) and the same bulk batch was used throughout this study. The following powders were used as filler materials and the assayed values estimated with correction for

moisture content ( $A_s$ ), the moisture contents ( $M_s$ ), and original sources were as follows; ZnO ( $A_s$ ; 99.9%,  $M_s$ ; 0.1%, Sakai Chemical Industry Co., Ltd.), TiO<sub>2</sub> ( $A_s$ ; 99.6%,  $M_s$ ; 0.2%, Titan Kogyo K.K.), StMg ( $A_s$ ; 4.4%,  $M_s$ ; 0.1%, Nippon Oil & Fats Co., Ltd.), talc ( $M_s$ ; 2.2%, Nippon Talc Co., Ltd.), SiAl ( $M_s$ ; 13%, Kyowa Chemical Industry Co., Ltd.). These powders satisfied the requirements of JP XI. Cp ( $A_s$ ; 100.4% converted for SiO<sub>2</sub>,  $M_s$ ; 2.2%, Shionogi & Co., Ltd.), and fine glass beads (GMB-04; average particle diameter: 40  $\mu\text{m}$ ,  $M_s$ ; 0%, Nippon Rikagaku Kikai).

**Preparation** The powder-filled semisolids were prepared on a 100 g scale as follows: the necessary amount of vaseline was weighed into a 200 ml beaker, and melted at 80 °C, then a powder was added. The mixture was agitated rapidly using an Ultra-turrax mixer (about 8000 rpm), and the powder was dispersed uniformly for 30 min, then the mixture was cooled to about 50 °C in 10 min under mild agitation in the Ultra-turrax mixer (about 4500 rpm). At about 50 °C, where the mixture became a little viscous, it was degassed under vacuum and the cooling to room temperature was continued under vacuum without agitation. After this degassing procedure, it was visually confirmed that bubbles had disappeared in the vaseline preparation (without powder). In the cases of powder-filled semisolids, it was difficult to assess visually whether they contained bubbles or not, so the same procedure was adopted for all ointment preparations as for the vaseline preparation.

The densities of the obtained powder-filled semisolids were measured on samples taken from upper, middle, and lower positions and were the same within the experiment error ( $CV\%$  was less than 0.5%). This suggested that the powders were uniformly dispersed in the semisolid.

The obtained semisolids were allowed to stand at 25 °C for more than a week to attain rheological equilibrium before the measurement. To establish the period required for the ointment to attain rheological equilibrium, measurements of the rheological properties of vaseline were performed previously, for more than a month. Equilibrium was attained within 3 d after preparation at 25 °C and thereafter the rheological parameters hardly changed. Therefore, standing for more than a week at 25 °C seemed to be enough for the vaseline-based ointments to attain equilibrium.

**Rheological Measurement** Oscillation measurement was carried out at 25 °C using a Shimadzu RM-1 rheometer as described previously<sup>2)</sup> [cone angle ( $\epsilon$ ),  $7 \times 10^{-2}$  rad; strain amplitude ( $\lambda$ ),  $1.75 \times 10^{-2}$  rad; radius of cone-and-plate ( $R$ ), 2.5 cm; torsion constant of wire ( $K$ ),  $2.22 \times 10^6$  dyn cm/rad; sample weight, about 3 g]. Rheological parameters  $G'$ ,  $G''$ ,  $\tan \delta$  and  $D_{nl}$  were calculated by using Eq. 1–4, respectively.

$$G' = (3Ka_1/2\pi R^3)(\epsilon/\lambda) \quad (1)$$

$$G'' = (3Kb_1/2\pi R^3)(\epsilon/\lambda) \quad (2)$$

$$\tan \delta = G''/G' \quad (3)$$

$$D_{nl} = \left( \int_0^{2\pi} |\sigma_{\text{obs}} - \sigma_{\text{1st}}| d\theta \right) / \left( \int_0^{2\pi} |\sigma_{\text{obs}}| d\theta \right) \quad (4)$$

Continuous shear measurement was performed as reported previously using a Ferranti-Shirley viscometer.<sup>2)</sup> The coefficients of variance of  $G'$ ,  $G''$ , apparent viscosity at 625 s<sup>-1</sup> ( $\eta_{625}$ ), and static yield values ( $SYV$ ) evaluated using vaseline were 6%, 7%, 5% and 5%, respectively.<sup>5)</sup> As the rheological parameters changed greatly upon addition of the powders, these variations were small enough for the purpose of this study.

In both methods, measurements were performed at 10 min after applying the samples to the rheometers. The rheological parameters were calculated from the first measurement because they usually altered with repeated application of shear.

**Powder Properties** Density ( $\rho$ ), bulk density ( $\rho_{\text{bulk}}$ ), specific surface area by the air permeability method ( $S_{\text{AP}}$ ) and BET method ( $S_{\text{BET}}$ ), and particle size ( $D_{\text{CL}}$ ) were determined as follows:

$\rho$ : An Autopycnometer 1320 (Micromeritics/Shimadzu Co., Ltd.) was used.

$\rho_{\text{bulk}}$ : In a 100 ml graduated cylinder, a powder was fed at a constant rate from 2 cm height from the edge of the graduated cylinder, then the weight of the powder was measured.

$S_{\text{AP}}$ : An apparatus for the measurement of specific surface area (type SS-10, Shimadzu Co., Ltd.) was used.

$S_{\text{BET}}$ : An Accusorb 2100E (Micromeritics/Shimadzu Co., Ltd.) was used (degas temperature, 120 °C; degas time, 17 h; vacuum, <0.1 mmHg).

$D_{\text{CL}}$ : Laser granulometry (Granulometer model 715, Cilas Co., Ltd.) was used with water. Ultrasonic irradiation was continued until stable distribution patterns were obtained (about

1 min).

**Wettability with Liquid Paraffin** Powders were packed into glass capillary tubes (diameter = 3.6 mm, length = 15 cm), then one end of the capillary tubes was stood in liquid paraffin at 25 °C. The rising liquid height ( $h$ ) in the tube was measured at appropriate time intervals. The slope was calculated from Eq. 5 by plotting  $h^2$  vs. time ( $t$ ).

$$h^2 = (\gamma_1 r \cos \theta) t / (2\eta) \quad (5)$$

where  $\gamma_1$ ,  $r$ ,  $\eta$ , and  $\theta$  are surface tension, average capillary radius, viscosity of liquid paraffin, and contact angle, respectively.

## Results and Discussion

**I) Properties of Powders Used** The powder properties,  $\rho$ ,  $\rho_{\text{bulk}}$ ,  $S_{\text{AP}}$ ,  $S_{\text{BET}}$ , and  $D_{\text{CL}}$ , are shown in Table I for the powders used in this experiment. In addition, the diameters of the particles were calculated from  $S_{\text{AP}}$  and  $S_{\text{BET}}$  by the use of Eqs. 6 and 7 on the assumption that all particles are uniform spheres.

$$D_{\text{AP}} = 6 \times 10^{-4} / (S_{\text{AP}} \times \rho) \quad (6)$$

$$D_{\text{BET}} = 6 \times 10^{-4} / (S_{\text{BET}} \times \rho) \quad (7)$$

Then, the following values were also calculated.

$$R_{\text{A/B}} = D_{\text{AP}} / D_{\text{BET}} \quad (8)$$

$$R_{\text{C/B}} = D_{\text{CL}} / D_{\text{BET}} \quad (9)$$

$S_{\text{AP}}$  is the specific surface area of powder calculated from the permeating time of air through the capillary tubes formed in powder beds. Therefore, the surface of closed tubes would not contribute to the surface area determined by this method. On the other hand, as the BET method estimates the whole surface including closed pores,  $R_{\text{A/B}}$  should take a larger value with increasing roughness of the surface of powders. The Cilas method counts an agglomerated particle as one particle, so  $R_{\text{C/B}}$  should be larger with increase of agglomeration.  $R_{\text{A/B}}$  and  $R_{\text{C/B}}$  are also shown in Table I.

From a comparison of the properties of powders shown in Table I, the powders can apparently be classified into 3 groups as follows. 1) High density powders (ZnO and TiO<sub>2</sub>):  $\rho$  and  $\rho_{\text{bulk}}$  are large and  $S_{\text{AP}}$ ,  $S_{\text{BET}}$  are small, although  $D_{\text{CL}}$  is small. In addition,  $R_{\text{A/B}}$  and  $R_{\text{C/B}}$  are not large, and therefore these powders should have a smooth surface and small degree of agglomeration. 2) Porous and bulky powders (Cp and SiAl):  $\rho$  takes a moderate value but  $\rho_{\text{bulk}}$  is very small, and  $S_{\text{BET}}$  and  $S_{\text{AP}}$  are very large. From the large  $R_{\text{A/B}}$  and  $R_{\text{C/B}}$  values, these powders would have very rough surfaces and many closed pores. Many fines should coagulate to form larger particles. 3) Powders used as lubricants (talc and StMg): they have almost the same particle sizes as those of group 2, but  $S_{\text{BET}}$ s are very much smaller than those of group 2. Based on the smaller  $R_{\text{A/B}}$  and  $R_{\text{C/B}}$  values, their surface should be smooth and

TABLE I. Properties of Powders Used in This Experiment

	$\rho$ (g/cm <sup>3</sup> )	$\rho_{\text{bulk}}$ (g/cm <sup>3</sup> )	$S_{\text{AP}}$ (m <sup>2</sup> /g)	$S_{\text{BET}}$ (m <sup>2</sup> /g)	$D_{\text{CL}}$ ( $\mu\text{m}$ )	$R_{\text{A/B}}$	$R_{\text{C/B}}$
ZnO	5.74	0.46	1.57	3.33	1.1	2.12	3.50
TiO <sub>2</sub>	3.97	0.52	2.85	8.93	0.6	3.13	3.55
Cp	2.81	0.09	10.40	145.40	13.0	13.98	885.24
SiAl	2.41	0.17	5.52	417.05	11.1	75.55	1859.42
StMg	1.10	0.26	1.69	4.69	15.6	2.78	13.41
Talc	2.82	0.40	1.23	2.17	12.9	1.76	13.16

agglomeration should be little.

**II) Evaluation by Oscillation Method** **1) Change in Viscoelastic Properties with Frequency ( $\omega$ )** Viscoelastic properties measured by the oscillation method are known to change greatly depending on many factors such as cone angle, maximum strain, and frequency. In addition, most of the ointment vehicles show nonlinear behavior. These features have made the rheological evaluation of ointments very complex. Thus many researchers have sought out a linear region between strain and stress, then determined the rheological parameters.<sup>6)</sup> According to the basic concept of viscoelastic theory, their procedure should be correct, but it is very troublesome to find a linear region for many ointments of various types, especially in the range of low shear rate. Further, such a procedure limits the rheological evaluation of ointments only to the linear region.

On the other hand, the extent of nonlinearity itself represents useful rheological information about ointments, because nonlinearity might reflect the thixotropic properties of ointments.<sup>2)</sup> In this experiment, maximum strain and cone angle were fixed, but the frequency ( $\omega$ ) was changed. Therefore,  $Dnl$  in Eq. 4 should be important for the examination of linearity. Figure 1 shows the  $\omega$  dependencies of  $G'$ ,  $\tan \delta$ , and  $Dnl$  for the ointment vehicles containing 10% (w/w) of ZnO, Cp, and StMg in vaseline compared with the control (vaseline).

As shown in Fig. 1A,  $\log G'$  increased with increase of  $\omega$  in all cases in the higher  $\omega$  range. In the lower  $\omega$  range,  $G'$  values of vaseline decreased with increase of  $\omega$  whereas  $G'$  values increased in other ointments. In the range where  $\log \omega$  was larger than  $-2$ , the order of  $G'$  values was  $Cp > ZnO > vaseline > StMg$ . It is very interesting that  $G'$  values of StMg were lower than those of vaseline in the whole  $\omega$  range.

The dependency of  $\log(\tan \delta)$  on  $\omega$  is shown in Fig. 1B. The values were larger than 0 ( $\tan \delta > 1$ ) in all cases. This means that the contribution of the liquid property to the viscoelasticity was larger than that of the solid property. As  $\omega$  increased,  $\tan \delta$  increased in all powders, reached a maximum, and then decreased. The reduction of  $\tan \delta$  with increase of  $\omega$  in the higher  $\omega$  range can be explained in terms of the Maxwell model by considering that the liquid element represented by a dash-pot can not follow a rapid oscillation whereas the solid element represented by a spring can react to the rapid oscillation. The reason why  $\tan \delta$  increased in lower  $\omega$  cannot be explained well physically, but this might be related to a greater thixotropic

property of all ointments as shown by high  $Dnl$  values in the low  $\omega$  range (Fig. 1C). The four semisolids in this experiment individually showed specific  $\tan \delta$  patterns and these patterns may be used for the identification of each semisolid as proposed by Davis.<sup>6a)</sup>

The  $Dnl$  values monotonously decreased with increase of  $\omega$  in all cases. According to the concept of the rheological ground state, the state at lower  $\omega$  should be near to the static state, but the contributions of nonlinear waves were very high in the lower  $\omega$  region. Evaluation of viscoelastic properties at low  $\omega$  where  $Dnl$ s are fairly high is undesirable even though it approaches the static state, because viscoelastic parameters ( $G'$ ,  $G''$ , and  $\tan \delta$ ) are principally calculated on the basis of a linear relation between strain and stress. Thus, in the following experiments, all determinations were performed at  $\omega = 0.47$  rad/s, where the  $Dnl$  values were the smallest.

**2) Influence of the Powder Species and Their Amounts**

Figure 2 shows the relative  $G'$  and  $G''$  values of powder-filled semisolids defined as:

$$G'_R = G' \text{ of powder-filled semisolid} / G' \text{ of vaseline} \tag{10}$$

$$G''_R = G'' \text{ of powder-filled semisolid} / G'' \text{ of vaseline} \tag{11}$$

As shown in Fig. 2A, the patterns of  $\log G'_R$  plotted against weight fraction of powders ( $f_p$ ) can be roughly classified into 3 types as follows: 1) ZnO;  $\log G'_R$  increased monotonously with increasing  $f_p$ , 2) Cp, SiAl;  $\log G'_R$  increased abruptly after a smaller change of  $\log G'_R$ , and 3) StMg, TiO<sub>2</sub>, and talc;  $\log G'_R$  decreased once, then increased gradually with increasing  $f_p$ . In the case of glass beads used as a control, the critical  $f_p$  value observed in most powders was not observed.

The decrease of  $G'_R$  observed in many powders at lower  $f_p$  might reflect interference by the particles with the formation of elastic structure of vaseline itself in the preparation procedure. Further, the lower  $G'_R$  in glass beads and StMg would reflect the difficulty in forming bridge structures in those cases.

As to  $\log G''_R$ , the values were not as changeable as those of  $\log G'_R$ , and tended to increase with increase of  $f_p$  for all powders except glass beads.

**3) Application of the Kerner Equation** The rheological properties of viscoelastic materials involving powder particles dispersed in a liquid or semisolid have been studied in many fields and various empirical or theoretical equations have been proposed.

An equation for the viscosity of a suspension was proposed by Einstein as:

$$\eta/\eta_0 = 1 + k_e \phi_2 \tag{12}$$

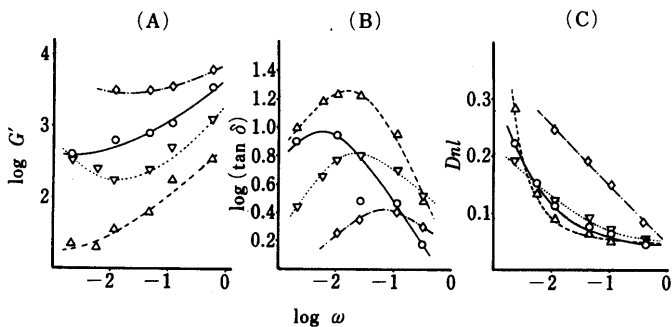


Fig. 1.  $\omega$  Dependencies of Storage Modulus ( $G'$ ; A), Loss Tangent ( $\tan \delta$ ; B), and Nonlinearity ( $Dnl$ ; C) of Powder (10%)-Filled Semisolids (○), ZnO; (△), StMg; (◇), Cp; (▽), vaseline.

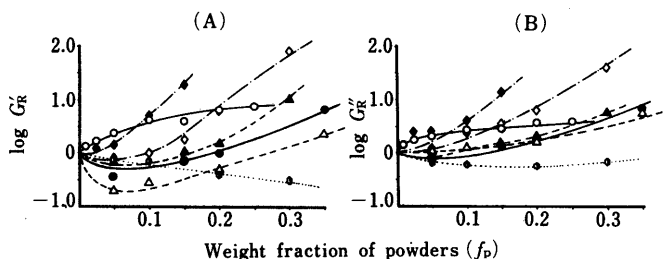


Fig. 2. Variation of  $G'_R$  and  $G''_R$  with Weight Fraction of Powders (○), ZnO; (●), TiO<sub>2</sub>; (△), StMg; (▲), talc; (◇), SiAl; (◆), Cp; (●), glass beads.

where  $k_e$  and  $\phi_2$  are a constant and the volume fraction of the dispersed material, respectively.

For more concentrated dispersions, Mooney modified Eq. 12 by using maximum volume fraction,  $\phi_m$  as follows<sup>7)</sup>:

$$\ln(\eta/\eta_0) = k_e \phi_2 [1/(1 - \phi_2/\phi_m)] \quad (13)$$

As to the equation for elasticity, Radebaugh and Simonelli reported the usefulness of the Kerner equation (Eq. 14) for a mixture in which the particles are sufficiently rigid compared with the vehicle.<sup>4)</sup>

$$G'_R = 1 + [15(1 - \mu_1)/(8 - 10\mu_1)](\phi_2/\phi_1) \quad (14)$$

where  $\mu_1$ ,  $\phi_2$  and  $\phi_1$  are Poisson's ratio of the bulk phase and the volume fractions of powder and vaseline, respectively.  $\phi_2$  and  $\phi_1$  were calculated by using Eqs. 15 and 16. In the following,  $\phi_1$  and  $\phi_2$  are denoted as  $\phi_{vas}$  and  $\phi_p$ , respectively, for easier recognition of the notation.

$$\phi_p = (f_p/\rho_p) / [f_p/\rho_p + (1 - f_p)/\rho_{vas}] \quad (15)$$

$$\phi_{vas} = 1 - \phi_p \quad (16)$$

where  $\rho_{vas}$  and  $\rho_p$  are the densities of vaseline and the powder, respectively.

Redebaugh and Simonelli applied this equation to powder-filled semisolids in which ZnO, potato starch, or colloidal sulfur was dispersed in lanolin and indicated that Eq. 14 did not agree with the experimental data in many cases but was useful to aid recognition of bridge structure formation by powders in semisolids, because Eq. 14 was derived under the assumption that there is good adhesion between the particles and the bulk phase, and the particles are rigid and spherical.

They suggested that  $G'_R$  should deviate to lower values in the case where slippage occurs under shear, and  $G'_R$  should deviate upward from the theoretical values in the case where bridge structures are formed in the semisolid. In Fig. 3,  $G'_R-1$  is plotted against  $\phi_p/\phi_{vas}$  according to Eq. 14.

Magnesium stearate showed lower values than the theoretical values (Fig. 3). The  $\mu_1$  value in Eq. 14 was set at 0.5 according to Radebaugh and Simonelli at low  $\phi_p/\phi_{vas}$  and the occurrence of slippage at the particle-bulk phase interface was presumed.<sup>4)</sup> In Cp, SiAl, TiO<sub>2</sub>, and talc,  $G'_R-1$  showed values close to the theoretical ones at low  $\phi_p/\phi_{vas}$ , but deviated upwards when  $\phi_p/\phi_{vas}$  was high. This could suggest the existence of bridge structures formed by powders whereby the ends of molecules in the vaseline phase interact with the surface of suspended particles and link

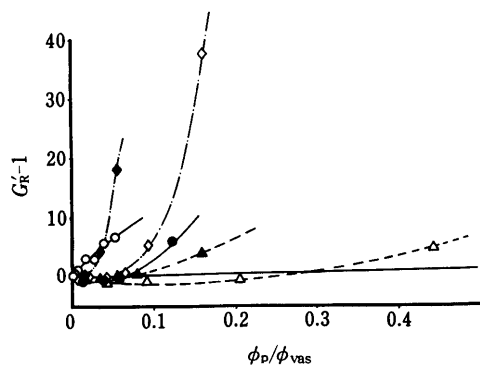


Fig. 3. Plot of  $G'_R$  According to the Kerner Equation  
(○), ZnO; (●), TiO<sub>2</sub>; (△), StMg; (▲), talc; (◇), SiAl; (◆), Cp.

different particles together.<sup>4)</sup> In ZnO,  $G'_R-1$  deviated upward and this suggested that the bridge structure is formed even at low  $\phi_p/\phi_{vas}$ . This could be because the powder contact of ZnO would be increased since ZnO has a very small particle size and shows good dispersion in vaseline.

**4) Loss Tangent** If particles are rigid enough and no special interactions occur between the vaseline phase and particles, the loss tangent,  $\tan \delta (=G''/G')$ , can be written as<sup>4)</sup>:

$$(G''/G')_{pfs} = (G''/G')_p \phi_p + (G''/G')_{vas} \phi_{vas} \quad (17)$$

where  $(G''/G')_{pfs}$ ,  $(G''/G')_p$ , and  $(G''/G')_{vas}$  mean the loss tangent of powder-filled semisolid, solid particles, and vaseline, respectively.

As  $G' \gg G''$  in a solid,  $(G''/G')_p$  is negligibly small and Eq. 17 can be written as:

$$(G''/G')_{pfs} = (G''/G')_{vas} \phi_{vas} = (G''/G')_{vas} (1 - \phi_p)$$

$$(G''/G')_{pfs} / (G''/G')_{vas} = 1 - \phi_p \quad (\tan \delta)_R = 1 - \phi_p \quad (18)$$

here,  $(\tan \delta)_R = (G''/G')_{pfs} / (G''/G')_{vas}$

To assess the applicability of Eq. 18,  $\log (\tan \delta)_R$  was plotted against  $\phi_p$  (Fig. 4). In Fig. 4,  $\log (\tan \delta)_R$  significantly deviated from Eq. 18 (in Fig. 4,  $\log (\tan \delta)$  calculated on the basis of Eq. 18 is shown as a line for comparison). Powders gave individual patterns, but showed a common tendency except for ZnO. That is, with increasing  $\phi_p$ ,  $(\tan \delta)_R$  increased, reached a maximum value, and then decreased. The peaks were observed at  $\phi_p$  of around 0.02—0.04 for most powders. However, in Cp, the peak

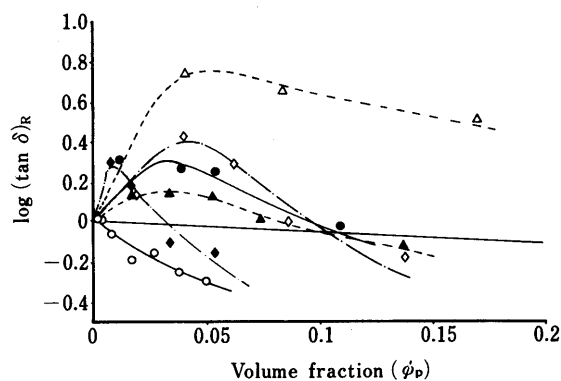


Fig. 4. Influence of the Volume Fraction of Powders on Loss Tangent  
The symbols are the same as in Fig. 3.

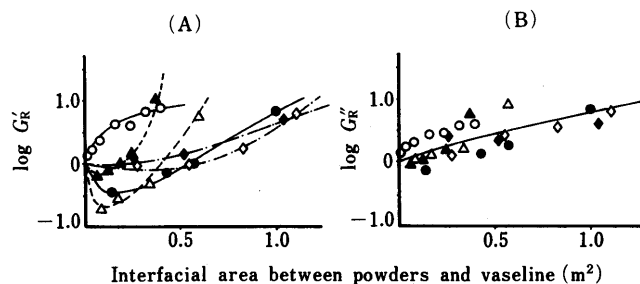


Fig. 5. Dependency of  $G'$  and  $G''$  Values on the Interfacial Area Calculated through  $S_{AP}$   
The symbols are the same as in Fig. 3.

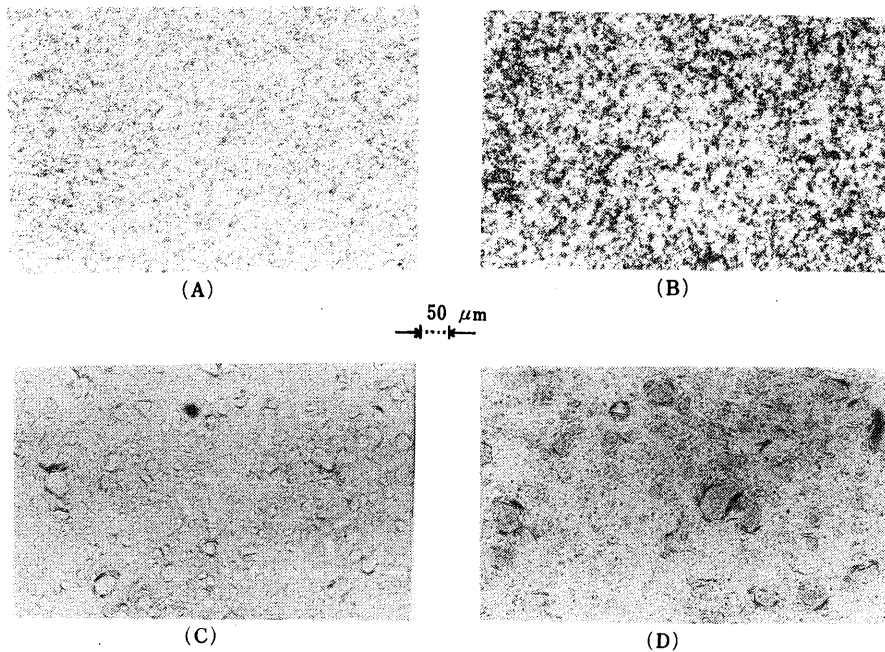


Fig. 6. Microphotographs of Representative Powder (10%-Filled Semisolids ( $\times 200$ )) (A), ZnO; (B),  $\text{TiO}_2$ ; (C), Cp; (D), SiAl.

was observed at a lower  $\phi_p$  of around 0.01. In the case of ZnO, the peak was scarcely observed and the curve fell monotonously. The decrease of  $(\tan \delta)_R$  reflects a relative increase of elasticity, and therefore it should reflect the formation of rigid structure in the powder-filled semisolid owing to the increase in the possibility of powder contact. Therefore, the  $\phi_p$  value corresponding to the peak of  $(\tan \delta)_R$  might reflect the beginning of structure formation.

The increase in  $(\tan \delta)_R$  observed at low  $f_p$  reflects the fact that  $G''$  values increased although  $G'$  values did not increase or decreased in most of the powders (Fig. 2).

**5) The Effect of the Interfacial Area** According to the Kerner equation (Eq. 14),  $G'_R$  should depend only on the volume fraction of powders and not on the powder species; however, as shown in Fig. 3, it differed greatly depending on the powder species. On the other hand, the viscosity of a dispersion is known to be fairly significantly affected by the interfacial area of dispersed particles.<sup>8)</sup> Thus, the relationship between interfacial area of powders and  $G'$  or  $G''$  was investigated.

For the specific surface area of powders, two kinds of values,  $S_{AP}$  and  $S_{BET}$ , were obtained from Table I.  $S_{AP}$  seemed to reflect the effective surface area of powders, because  $S_{BET}$  was obtained by measuring the whole capillary tube surface. Specific area can also be calculated using the mean diameter obtained by the Cilas method (denoted as  $S_{CL}$ ). However,  $S_{CL}$  might not reflect the interfacial surface area between particles and vaseline, because water was used as the dispersion medium in the Cilas method. The extent of agglomeration of the powders might differ greatly between the measuring medium and hydrophobic vaseline. (An agglomerated mass was counted as one particle by this method, and this might result in a discrepancy between  $S_{CL}$  and the real interfacial surface area.)

Thus,  $G'_R$  and  $G''_R$  were plotted in Fig. 5A and B, respectively, against interfacial area calculated by Eq. 19

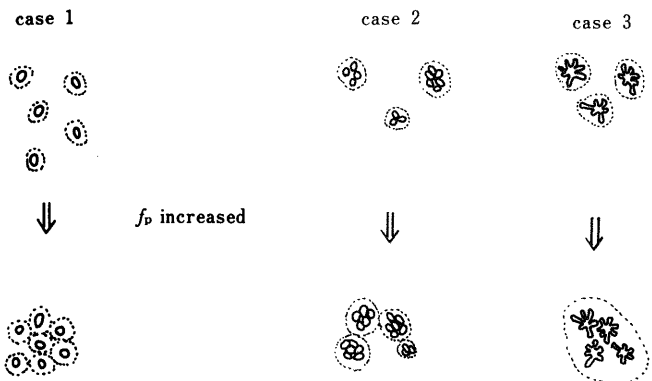


Fig. 7. Schematic Representation of Three Types of Presumptive Bridge Structures Formed by Powders

In the figure, the dotted lines represent the semisolid layer adhering to the solid particles.

under the assumption that the interfacial areas were equal to the surface areas of the powders determined by the air permeability method.

interfacial area (per powder-filled semisolid, 1 g)

$$= S_{AP} \times f_p \tag{19}$$

$G''_R$  increased with interfacial area irrespective of powder species and seemed to be considerably influenced by interfacial area (Fig. 5B). However, the finding that  $G'_R$  showed various patterns (Fig. 5A) could not be understood through the effect of interfacial area alone. The nature of bridge structures formed by powders may influence the  $G'_R$  patterns.

**6) Discussion of Factors Affecting  $G'_R$**  Microphotographs of representative powder-filled semisolids are shown in Fig. 6. From the pictures and the preceding results, three types of bridge structure formed by the powders could be identified, as shown schematically in Fig. 7.

In case 1, particles were separate from each other and the structure was formed through the contact of individual particles with increasing  $f_p$ . In case 2, particles were agglomerated even at low  $f_p$  and the bridge structures were formed through increasing agglomeration with increasing  $f_p$ . In case 3, powder particles had many protuberances and the structures were formed through the entanglement of the protuberances of particles. Case 3 might be regarded as a special case of case 2 if the rough surfaces of Cp and SiAl were formed through the agglomeration of very fine particles.

From microscopic observations, ZnO (Fig. 6A), StMg, and talc seemed to be dispersed in accordance with case 1. TiO<sub>2</sub> (Fig. 6B) seemed to belong to case 2, and porous powders [Cp (Fig. 6C) and SiAl (Fig. 6D)] seemed to be classified as case 3.

The density of powder-filled semisolids could help in their recognition. By use of the densities in Table I, the void volume in the powder-filled semisolid,  $\epsilon_p$ , could be calculated from the following relation:

$$\epsilon_p = 1 - f_p / [\rho_p \{1/\rho_{pfs} - (1-f_p)/\rho_{vas}\}] \quad (20)$$

where  $\rho_{pfs}$  means the observed density of the powder-filled semisolid.

The  $\epsilon_p$  values at 20% powder concentration were calculated and are shown in Table II. The  $\epsilon_p$ s of ZnO, talc, and StMg were near to zero, whereas those of Cp, SiAl, and TiO<sub>2</sub> were fairly high.

Among powders having high  $\epsilon_p$  values, Cp and SiAl had high  $R_{A/B}$  and  $R_{C/B}$  values (Table I). However, TiO<sub>2</sub> did not have such high  $R_{A/B}$  and  $R_{C/B}$  values, and therefore it was expected that TiO<sub>2</sub> should have similar patterns in the relations between  $\log G'_R$  vs.  $f_p$ , and  $\log (\tan \delta)_R$  vs.  $f_p$  to those of ZnO. However, TiO<sub>2</sub> gave very different patterns from ZnO. In fact, it was observed microscopically that particles of TiO<sub>2</sub> were agglomerated with each other in vaseline and formed fairly large masses (Fig. 6B), whereas ZnO was dispersed well in vaseline (Fig. 6A). The reason could be the difference in affinity for vaseline, evaluated in terms of the wettability. As shown in Table II, TiO<sub>2</sub> showed very low  $r \cos \theta$  values with liquid paraffin and this suggested that TiO<sub>2</sub> has poor wettability with such mineral oils. The high  $\epsilon_p$  value of TiO<sub>2</sub> shown in Table II implies that vaseline could not penetrate into the voids formed in the agglomerated TiO<sub>2</sub> mass. As to Cp and SiAl, the high  $\epsilon_p$  values might reflect both intra- and interparticle voids because they had large closed void volumes, as is clear from the small  $R_{A/B}$  values, and seemed to agglomerate easily through the entanglement of rough surfaces.

If particles had analogous powder properties (density, surface state, etc.) except particle size, the particle sizes of powders should be correlated with the volume fraction

TABLE II.  $\rho_{pfs}$ ,  $r \cos \theta$ , and  $\epsilon_p$  Obtained for the Powders Used

	ZnO	TiO <sub>2</sub>	Cp	SiAl	StMg	Talc
$\rho_{pfs}$	1.085	1.041	0.985	1.006	0.934	1.046
$\epsilon_p$	0.025	0.325	0.278	0.232	0.016	0
$r \cos \theta (\times 10^4)$	8.5	0.01	5.3	6.0	9.1	5.0

$\rho_{pfs}$ : density of powder filled semisolids.  $\epsilon_p$ : porosity of powders filled semisolids.  
 $r \cos \theta$ : wettability of powders by liquid paraffin.

$\phi_{p \max}$  at which  $\tan \delta$  showed the maximum value and this would correspond to the beginning of structure formation. The smaller particles should begin structure formation at low  $f_p$  and should give smaller  $\phi_{p \max}$ .

ZnO particles were very small, as shown in Table I, and dispersed well in vaseline; therefore,  $\phi_{p \max}$  should be near to 0. TiO<sub>2</sub> should show the lowest  $\phi_{p \max}$  because the particle size was the smallest, but  $\phi_{p \max}$  was 0.03 and fairly large compared with that of ZnO. The reason was discussed above. As to Cp and SiAl,  $D_{CL}$  took almost the same values. However, particles of Cp were seen to be smaller in the powder-filled semisolid by microscopic observation (Fig. 6C and D) and they might have been divided into smaller particles during the preparation of the powder-filled semisolid, because Cp seemed to be very fragile as presumed from the low  $\rho_{bulk}$ . This might be the reason why  $\phi_{p \max}$  of Cp was smaller than that of SiAl.

As to talc and StMg,  $\phi_{p \max}$  seemed to be around 0.04–0.1 in both cases, but was less distinct than with the other powders. However, bridge structure seemed to be formed more easily by talc than by StMg as indicated by the higher  $G'_R$  and  $G''_R$  values shown in Fig. 2. This might be related to the fact that StMg has a more effective lubricant function than talc. Therefore, slippage between particles might occur more frequently in StMg, and bridge structure would hardly be formed at lower  $f_p$  as in the case of glass beads.

7) Determination by the Continuous Shear Method  
 The structure formed in vaseline seemed to be affected by

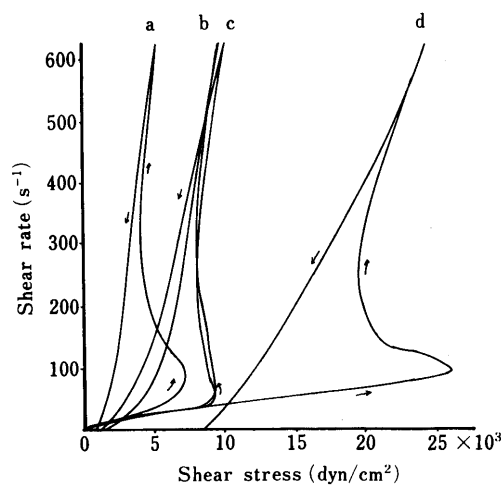


Fig. 8. Continuous Shear Rheograms of Powder (10%) Filled Semisolid  
 Powder in semisolid: (a), none (vaseline alone); (b), ZnO; (c), StMg; (d), Cp.

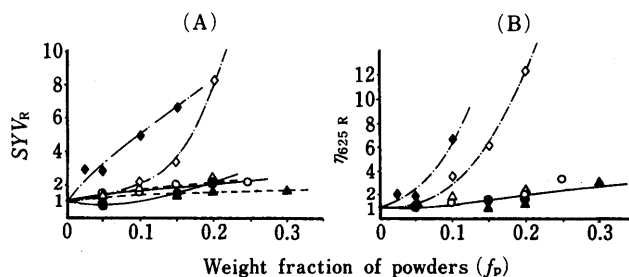


Fig. 9. Influence of  $f_p$  on  $SYR$  and  $\eta_{625 R}$  Determined with a Ferranti-Shirley Viscometer

The symbols are the same as in Fig. 3.

many factors for each powder, as described above. By the evaluation of rheological properties in the rheological ground state, information on the structures in a nearly static state could be obtained. However, many of these structures would be destroyed at higher shear rate and the behavior of residual structures at higher shear rate is also important for an understanding of the structures of powder-filled semisolids. Thus, rheological evaluation was also done by the continuous shear method using a Ferranti-Shirley viscometer. Figure 8 shows representative rheograms of powder-filled semisolids.

All of the powder-filled semisolids showed higher shear stress than vaseline alone. In all cases, spur points which correspond to static yield values ( $SYV$ ) were observed.

Figure 9 shows the relative value of  $SYV$  and the relative apparent viscosity at the shear rate of  $625\text{ s}^{-1}$  ( $\eta_{625}$ ) with respect to those of vaseline ( $SYV_R$  and  $\eta_{625R}$ , respectively) against  $f_p$ .

The relative value of static yield should represent the resistance of the structure in powder-filled semisolids to shear.  $SYV_R$  values were increased greatly by addition of Cp, and SiAl, and scarcely increased by other powders. Thus,  $SYV_R$  of ZnO and talc showed a very different tendency from the  $G'_R$  values (Fig. 2A), since  $G'_R$  increased considerably at higher  $f_p$ . This suggests that the bridge

structures of these powders formed in the static state are very fragile.

The  $\eta_{625R}$  values were also greatly increased by Cp and SiAl, but were not so much affected by other powders. It is very interesting that porous powders such as Cp and SiAl have a marked effect on  $G'_R$ ,  $SYV_R$ , and  $\eta_{625R}$ . This means that the structures formed by these powders through the entanglement of protuberances are strong in both static and shear-imposed states.

#### References

- 1) S. Onogi, T. Masuda and M. Matsumoto, *Trans. Soc. Rheol.*, **14**, 275 (1970).
- 2) M. Kobayashi, S. Ishikawa and M. Samejima, *Chem. Pharm. Bull.*, **30**, 4468 (1982).
- 3) S. Ishikawa, M. Kobayashi and M. Samejima, *Chem. Pharm. Bull.*, **36**, 2118 (1988).
- 4) G. W. Radebaugh and A. P. Simonelli, *J. Pharm. Sci.*, **73**, 590 (1984); *idem, ibid.*, **74**, 3 (1985).
- 5) M. Kobayashi, S. Ishikawa and M. Samejima, *Journal of Japanese Cosmetic Science Society*, **7**, 336 (1983).
- 6) a) S. S. Davis, *J. Pharm. Sci.*, **60**, 1351 (1971); b) G. M. Eccleston, B. W. Barry and S. S. Davis, *ibid.*, **62**, 1954 (1973); c) B. W. Barry and M. C. Meyer, *Int. J. Pharm.*, **2**, 27 (1979).
- 7) M. Mooney, *J. Colloid Sci.*, **6**, 162 (1951).
- 8) H. B. Kostenbauder and A. N. Martin, *J. APhA. Sci. Ed.*, **43**, 401 (1954).